Reversal of the tamoxifen-resistant breast cancer malignant phenotype by proliferation inhibition with bromosulfonamidine amino-podophyllotoxin

JIAYI WANG[1-3], FEN LV[2,3], YINGHUA ZHU[2,3], XIAOMEI LU[2,3] and BAO ZHANG[1]

[1]BSL-3 Laboratory (Guangdong), Guangdong Provincial Key Laboratory of Tropical Disease Research, School of Public Health, Southern Medical University, Guangzhou, Guangdong 510515, P.R. China; [2]Medical Laboratory (Guangdong), Dongguan Eighth People's Hospital, Dongguan, Guangdong 523320, P.R. China; [3]Department of Genetics, Key Laboratory for Children's Genetics and Infectious Diseases of Dongguan, Dongguan, Guangdong 523320, P.R. China

Received September 5, 2023; Accepted April 16, 2024

DOI: 10.3892/ol.2024.14506

Abstract. One of the lignans isolated from plants within the genus *Podophyllum* is podophyllotoxin (PPT). PPT and its derivatives are pharmacologically active compounds with potential antiproliferative properties in several kinds of tumors. Although these compounds have been used to treat other malignancies, no PPT derivative-based chemotherapeutic agent has been used to cure tamoxifen (TAM)-resistant breast cancer in clinical trials, to the best of our knowledge. Thus, using TAM-resistant breast cancer as a disease model, the present study assessed the effects of a recently synthesized PPT derivative, bromosulfonamidine amino-PPT (BSAPPT), on TAM-resistant breast cancer. Using the tamoxifen-resistant breast cancer cell model (MCF-7/TAMR) *in vitro*, Cell Counting Kit-8 and colony formation assays were adopted to evaluate the effect of BSAPPT on cell proliferation. Cell apoptosis and cell cycle assays were used to assess the influence of BSAPPT on cell apoptosis and the cell cycle in MCF-7/TAMR. The targets of the potential mechanism of action were analyzed by RT-qPCR and western blotting. The present study demonstrated that BSAPPT suppressed MCF-7/TAMR cell proliferation in a dose-dependent manner. By modulating the level of expression of genes linked to both apoptosis and the cell cycle, BSAPPT triggered MCF-7/TAMR cells to undergo apoptosis and prevented them from entering the cell cycle. Consequently, BSAPPT blocked these cells from proliferating, thereby halting the malignant advancement of TAM-resistant breast cancer. Therefore, these findings indicate that new therapeutic agents involving BSAPPT may be developed to facilitate the treatment of TAM-resistant breast cancer.

Correspondence to: Professor Bao Zhang, BSL-3 Laboratory (Guangdong), Guangdong Provincial Key Laboratory of Tropical Disease Research, School of Public Health, Southern Medical University, 1023-1063 Shatai South Road, Baiyun, Guangzhou, Guangdong 510515, P.R. China
E-mail: zhang20051005@126.com

Professor Xiaomei Lu, Medical Laboratory (Guangdong), Dongguan Eighth People's Hospital, 68 West Lake Third Road South, Shilong, Dongguan, Guangdong 523320, P.R. China
E-mail: luxm@dgp-institute.com

Key words: bromosulfonamidine amino-podophyllotoxin, tamoxifen-resistant breast cancer, etoposide, apoptosis, cell cycle

Introduction

Breast cancer is the most common malignancy in women and is an imminent threat to the health and lives of women; according to a World Health Organization report, 2.1 million women are affected by breast cancer each year. It was reported that 627,000 women died due to breast tumors in 2018 (1,2). Furthermore, it has the worst morbidity and mortality rates among all female-associated malignancies worldwide, with the latest data showing that breast cancer accounts for 24.5% of global female cancer morbidities and 15.5% of associated mortalities (3).

Estrogen receptor (ER) positivity is present in 70% of patients with breast cancer (4). To suppress ER-mediated mitogenic estrogen signaling, tamoxifen (TAM), a particular ER modulator, competes with estrogen for its ER ligand-binding domain (1). TAM has known therapeutic effects against ER^+ breast carcinoma (1,5). TAM (an endocrine therapy) mitigates the recurrence rate of early-stage ER^+ breast cancer by ~40%; nevertheless, TAM resistance develops in ~30% of such patients after ongoing therapy, leading to tumor recurrence and metastasis (6). TAM resistance is the primary cause contributing to treatment failure in patients who have ER^+ breast carcinoma; however, few treatment options are currently available (7). Therefore, investigating efficacious strategies for TAM-resistant breast cancer is imperative.

Breast cancer resistance to TAM abnormally enhances malignant phenotypes, such as metastasis, proliferation, invasion, resistance to apoptosis and chemotherapy tolerance (7-9). Through the PI3K/AKT/mTOR signaling process, ER^+ breast tumor cells have been shown to bypass the inhibitory properties of TAM to develop additional malignant phenotypes.

Growth factors stimulate the PI3K/AKT/mTOR signaling pathway by activating growth factor receptors such as human epidermal growth factor receptor 2, epidermal growth factor receptor, vascular endothelial growth factor or insulin-like growth factor. These factors enable the overexpression of anti-apoptotic genes [B-cell lymphoma (Bcl)-extra-large and *Bcl-2*], genes linked to migration [*Snail*, which induces epithelial-mesenchymal transition of tumor metastasis by binding to the E-box in the E-cadherin promoter region among epithelial tumors; *Twist*, which promotes the metastasis process in human breast tumor and it promotes breast cancer by downregulating E-cadherin and estrogen receptor; and *MMP9*, which is crucial in protein lysis and extracellular matrix remodelling, and is related to tumor metastasis, invasion and regulation of the tumor microenvironment] and genes related to the cell cycle (*Cyclin D1, CDK4/6* and *c-Myc*), thereby generating malignant phenotypes in the drug-resistant strain (7,10-18). Therefore, small-molecule drugs that inhibit cell proliferation by interfering with cell growth factors may overcome the malignant phenotype of MCF-7/TAMR cells.

Studies have reported that podophyllotoxin (PPT) is derived from different species of PPT rhizomes, which are lignans isolated from plants of the genus *Podophyllum*. PPT and its derivatives are pharmacologically active (19,20). The widespread interest in lignans stems from their potent antiviral and antineoplastic properties (21). Microtubule protein polymerization is known to be blocked by PPT and its derivatives, which have anticancer characteristics, thereby halting the cell cycle at the G_2/M phase (22,23). This has attracted attention for pharmacological studies in recent decades with the invention of the semi-synthetic anticancer compound etoposide and teniposide, which have inspired long-term studies of this structural phenotype (24). To date, the two epiPPT derivatives have been developed as clinical therapeutic agents (24); they are chemotherapeutic agents in the treatment of myeloid leukemia, pancreatic malignancy, testicular cancer, gastric tumors, lymphoma and small-cell lung cancer (23,25).

Notably, the two medications have shown certain inhibitory effects on breast cancer cells at the cellular level (26,27). For example, to hinder cell proliferation, etoposide inhibits DNA topoisomerase II and stops the cell cycle at the S phase (19,21). Certain phase II clinical studies have reported the effectiveness of oral etoposide as a therapy for metastatic breast cancer. However, its widespread clinical use is yet to be confirmed by large-scale randomized controlled clinical studies (28). Etoposide is a genotoxic compound that occasionally causes severe side effects, including secondary leukemia, bone marrow suppression, gastrointestinal disorders, neutropenia and peripheral neuropathy. Presently, etoposide therapy for breast tumors is regarded as experimental. When etoposide is applied, cells can evade apoptosis, continue proliferating and become resistant to the drug (28-30). Furthermore, teniposide is a potent broad-spectrum antineoplastic drug that results in DNA damage during replication and the induction of apoptosis (31). Its minimal water solubility and unfavorable response to the marketed dose induce anaphylaxis and restrict its clinical feasibility (32). Anhydrous ethanol is often applied to increase water solubility. This has undesirable effects (anaphylaxis) and is not well tolerated by certain patients (33). Conversely, teniposide is free in VM-26, thus promoting swift clearance and broad tissue dissemination involving cancerous tissues and healthy organs, thereby decreasing its curative effectiveness and enhancing adverse reactions. Despite successfully halting the expansion of MCF-7 transplanted tumor models *in vivo*, teniposide micelles are not clinically useful (34,35).

Etoposide and teniposide often exhibit unexpected toxicity at effective doses in clinical trials, thereby limiting their clinical application. This has provided justified creation of novel PPT derivatives with reduced harmful *in vivo* effects and enhanced antineoplastic properties (21,36). Under these circumstances, structural modifications of the PPT backbone have been performed to synthesize novel, effective PPT compounds, including tafluposide, NPF, NK-611, TOP-53 and nitrogenous toxins. NK-611, which replaces the hydroxyl group with dimethyl in the sugar group of etoposide, inhibits TOP2 and is more effective than etoposide against some tumor cells *in vitro*. TOP-53 is more likely to cause chromosome breakage, is more effective than etoposide on non-small cell lung cancer cells, and shows extremely different drug resistance, anti-tumor spectrum and TOP2 inhibitory function from etoposide. NPF is a 100x more potent than etoposide against all cancer cells and can be used as a lead compound for further manufacturing of new antitumor drugs (21,25,37). A previous study reported that a nitroxyl spin-labelled derivative of podophyllotoxin (GP7) induced apoptosis in human leukemia cells (38). GP7 showed potent inhibitory effects on mouse and human osteosarcoma cells *in vitro*, and GP7 arrested the cell cycle at the S phase (38). Studies on any of the aforementioned PPT derivatives in the therapy of TAM resistance in breast cancer, however, are lacking.

The present study aimed to screen one of the derivatives, bromosulfonamidine amino-PPT (BSAPPT), that effectively targets TAM-resistant breast cancer cells, and to assess the role of BSAPPT in different types of tumor cell lines. Aside from breast cancer, lung cancer ranks second in terms of incidence among both men and women (11.4% of total cases), and it is the main cause of cancer-related deaths worldwide (18.0% of total cases). Therefore, it also warrants close attention (3,39). In the present study, CCK-8, colony formation, apoptosis, cell cycle, RT-qPCR and western blotting assays were used to detect the proliferation inhibition, apoptotic and cell cycle effects, and the molecular targets of BSAPPT on MCF-7, MCF-7/TAMR, A549 and MDA-MB-231 cancer cells.

Materials and methods

Cells and drugs. MCF-7 (human breast adenocarcinoma), MCF-10A (human normal mammary epithelial cells), A549 (human non-small cell lung cancer) and MDA-MB-231 (human breast adenocarcinoma) cell lines were purchased from the American Type Culture Collection Cell Bank. All cell lines used in the current study were identified by Shanghai Yihe Applied Biotechnology Co., Ltd., and matched exactly to the corresponding cell lines. Bromosulfonamidine amino-PPT (BSAPPT) was kindly donated by Dr Weiguang Yang of Guangdong Medical University (Zhanjiang, China) and stored in the laboratory.

Main reagents. FBS serum was purchased from Shanghai ExCell Biology, Inc. Trypsin, RPMI-1640 medium and

DMEM were purchased from Gibco (Thermo Fisher Scientific, Inc.). 4-hydroxytamoxifen was purchased from Sigma-Aldrich (Merck KGaA). The reverse transcription kit (cat. no. A0010CGQ), SYBR Green Premix Dye Real-Time Fluorescence Quantitative (q)PCR kits (cat. no. A0012-R2) and the total intracellular RNA extraction reagent (cat. no. B0004D) were purchased from EZBioscience. The kit for proliferation (Cell Counting Kit-8; cat. no. C6030) was purchased from NCM Biotechnology. Crystalline violet staining solution and 4% paraformaldehyde fixative were purchased from Beyotime Institute of Biotechnology. The assay kit for apoptosis (BD Pharmingen™ FITC Annexin V Apoptosis Detection Kit; cat. no. 556547) was purchased from BD Biosciences and the kit for the cell cycle test [Cell Cycle Assay Kit (Red Fluorescence); cat. no. E-CK-A351] was purchased from Elabscience Biotechnology, Inc. Mouse anti-human Caspase-9 antibodies (cat. no. 9508S; 1:1,000) were purchased from Cell Signaling Technology, Inc., rabbit anti-human Bcl-2 (cat. no. BA0412; 1:1,000) and cyclin B1 (CCNB1; cat. no. BA0766; 1:1,000) antibodies were purchased from Wuhan Boster Biological Technology, Ltd., rabbit anti-human polo like kinase (PLK)-1 antibodies (cat. no. 10305-1-AP; 1:1,000) and targeting protein for Xklp2 (TPX2) antibodies (cat. no. 11741-1-AP; 1:2,000) were purchased from Proteintech Group, Inc., and the rabbit anti-human PLK-4 antibodies (cat. no. A9863; 1:1,000) were purchased from ABclonal Biotech Co., Ltd. Mouse anti-GAPDH antibodies (cat. no. abs830030; 1:1,000) were purchased from Absin Bioscience, Inc. The UltraSignal hypersensitive ECL Chemiluminescence Substrate (cat. no. 4AW011-500) was purchased from Beijing 4A Biotech Co., Ltd. and the PVDF membranes (cat. no. FFP33) were purchased from Beyotime Institute of Biotechnology.

Cell culture. MCF-7 and MCF-7/TAMR cells were cultured in RPMI-1640 media containing 10% FBS in a constant-temperature incubator maintained at 37˚C with 5% CO_2. MCF-7/TAMR cells were obtained by cultivating MCF-7 in an estrogen-deprived environment with low-to-high TAM concentrations (100, 200, 500, 800 and 1,000 nM) for >6 months to ultimately form MCF-7/TAMR resistant to TAM at a concentration of 1 μM (7). MCF-10A cells were cultured in a specialized complete medium at 37˚C with 5% CO_2, whilst A549 and MDA-MB-231 cells were cultured in DMEM and RPMI-1640 media at 37˚C with 5% CO_2, respectively. Then these cells were passaged at 3-day intervals.

Morphological observation of cells. Cell death and floating conditions of MCF-7 and MCF-7/TAMR cells ($3x10^5$) treated with or without BSAPPT (10 μg/ml) at 37˚C for 48 h were observed under an inverted optical microscope using a 10X objective.

Reverse transcription-qPCR. Intracellular RNA was isolated from four types of cells, MCF-7, MCF-7/TAMR, A549 and MDA-MB-231, treated or untreated with BSAPPT, using the EZ-Press RNA Purification Kit (cat. no. B0004D; EZBioscience). Moreover, reverse transcription was performed using 1 μg total RNA to produce cDNA after determining a specific concentration using the Color Reverse Transcription Kit (with genomic DNA remover) (cat. no. A0010CGQ; EZBioscience). Reverse transcription was performed at 42˚C for 15 min and 95˚C for 30 sec. The relative expression levels of *Bcl-2,* Caspase-9, *PLK1*, *PLK4*, *CCNB1*, *TPX2* and β-actin genes were detected using SYBR Green dye. The qPCR procedure was as follows: 95˚C for 5 min for one cycle, followed by 95˚C for 10 sec and 60˚C for 30 sec for 40 cycles. The results were calculated using the $2^{-\Delta\Delta Cq}$ (40) method to obtain the ploidy of each target gene relative to β-actin. Table I lists the primer sequences.

Western blotting. To detect target proteins, MCF-7 and MCF-7/TAMR cells were added to two separate six-well plates with 250,000 cells per well, respectively. They were set up in two groups: One with added BSAPPT and one without BSAPPT. After 48 h, three wet washes at 4˚C using pre-cooled PBS were performed on the cells. Next, the mixed solution containing RIPA-strong lysis solution (Cowin Biotech Co., Ltd) and proteinase inbitor (Biosharp) (RIPA lysis solution: proteinase inhibitor, 100:1) was added to the cells, and the cells were lysed on ice for 15 min. The BCA (cat. no. P0010; Beyotime Institute of Biotechnology) assay was used to test the protein concentrations. Cells were then centrifuged at 4˚C and 16,099 x g for 15 min. The supernatant was collected and the 5X SDS-PAGE loading buffer (Beyotime Institute of Biotechnology) was added, then the cells were incubated in a metal bath at 100˚C for 10 min. Proteins (15 μg/lane) were separated on 10% gels using SDS-PAGE. The mixture was electrotransferred to a PVDF membrane and vibrated at room temperature (25˚C) for 1 h after being blocked with 5% skimmed milk powder (Fujifilm Wako Pure Chemical Corporation) at 25˚C for 1 h. Primary antibodies (GAPDH, Bcl-2, Caspase-9, PLK1, PLK4, CCNB1 and TPX2) were then added with diluted 5% BSA and refrigerated at 4˚C overnight. A total of three TBST (0.05% Tween-20) washes were performed on the membrane, 5 min each time, and then the membrane was incubated with the corresponding HRP-conjugated secondary antibodies (cat. no. BA1054; 1:5,000; Boster Biological Technology) for 2 h at 4˚C, followed by three 10-min washes. ECL reagent (4A Biotech, Co., Ltd.) was used for visualization of protein bands in fluorescence and chemiluminescence imaging systems (Clinx Science Instrume nts Co., Ltd.), and images were captured.

Cytotoxicity assay. MCF-7, MCF-7/TAMR, MCF-10A, A549 and MDA-MB-231 cells were each placed at an average density of 50,000 cells/well in 24-well plates to produce the control and treatment groups. A total of 500 μl complete media was added to each well. BSAPPT at a drug concentration gradient of 1, 5, 10, 20 and 40 μg/ml was added to the treatment group. MCF-7, MCF-7/TAMR and MCF-10A cells were separately added to three 24-well plates at 50,000/well and treated with etoposide at a concentration gradient of 1, 5, 10, 20, 40 and 80 μg/ml (MCF-7 and MCF-7/TAMR) or an etoposide concentration gradient of 1, 2.5, 5, 10, 20 and 40 μg/ml (MCF-10A). Prior to the assay, the old medium was removed from each well, washed with PBS at room temperature (25˚C), and refilled with fresh 380 μl media. Following the addition of 38 μl of CCK-8 solution, the culture plate was gently shaken. The mixture was incubated for 30 min at 37˚C in an incubator. Using a microplate reader, the absorbance of each well was measured at 450 nm.

Table I. Quantitative PCR primers.

Primer	Direction	Sequence (5'-3')
PLK1	F	CGAGTTCTTTACTTCTGGCT
	R	TATTGAGGACTGTGAGGGGC
CCNB1	F	GCACTTTCCTCCTTCTCA
	R	CGATGTGGCATACTTGTT
Bcl-2	F	GGTGGGGTCATGTGTGTGG
	R	CGGTTCAGGTACTCAGTCATCC
Caspase-9	F	GCAGTAACCCCGAGCCAGATG
	R	CCGGAGGAAATTAAAGCAACCAG
PLK4	F	AGTGCTCCCTTTTTCCCAAT
	R	AGCAGCACTATGCATGACCA
TPX2	F	ATGGAACTGGAGGGCTTTTTC
	R	TGTTGTCAACTGGTTTCAAAGGT
Bax	F	GGGGACGAACTGGACAGTAA
	R	CAGTTGAAGTTGCCGTCAGA
Cyt-C	F	AGGCCCCTGGATACTCTTACACA
	R	TCTGCCCTTTCTTCCTTCTTCTTA
Apaf-1	F	AATGGCAGGCTGTGGGAAGTC
	R	TAAGTGGAAGCCTCTGGGAAAAAC
Caspase-3	F	TGGCGAAATTCAAAGGATG
	R	TAACCCGGGTAAGAATGTGC
β-actin	F	CATGTACGTTGCTATCCAGGC
	R	CTCCTTAATGTCACGCACGAT

PLK, polo like kinase; CCNB1, cyclin B1; Bcl-2, B-cell lymphoma 2; Caspase, cysteine aspartic acid-specific protease; TPX2, targeting protein for Xklp2; Bax, Bcl-2 associated X; Cyt-C, cytochrome *c*; Apaf-1, apoptotic protease activating factor 1; F, forward; R, reverse.

Colony formation assay. A total of 500 MCF-7 and MCF-7/TAMR cells/well were added to two separate 6-well cell culture plates. BSAPPT was added at increasing dosages (1, 5, 10, 20 and 40 μg/ml). The medium was changed every three days during the incubation period at 37˚C of 7-14 days to monitor the condition of the cells. Under a inverted microscope, the number of colonies was counted, and when it reached an average of >50 cells in a colony, the cells were fixed for 15 min in 1 ml 4% polyformaldehyde at room temperature (25˚C) before being stained for an additional 15 min in 500 μl crystal violet staining solution (0.1%) at room temperature (25˚C). Colony counts were then performed by ImageJ software (version 1.8.0; National Institutes of Health).

Cell apoptosis assay. A total of 250,000 MCF-7, MCF7/TAMR, A549 and MDA-MB-231 cells were separately inserted in each well of four six-well plates. The control and experimental groups were set up concurrently. When cell growth reached 50-60%, a total of 5 μg/ml BSAPPT was separately added to the 4 types of cells in the experimental group at 37˚C for 48 h before the cell supernatant was collected; at the same time, the control group was replaced with fresh culture medium. After 48 h of cell culture, the cell supernatant of the control and treatment groups was collected. After trypsin digestion, all cells were collected and the six-well plates were rinsed with cold PBS, and after removing the supernatant by centrifugation at 800 x g and room temperature (25˚C) for 3 min, they were then washed twice using cold PBS before cell precipitates were resuspended with 500 μl 1X binding buffer ([10X Annexin V Binding Buffer, 0.1 M Hepes/NaOH (pH 7.4), 1.4 M NaCl and 25 mM $CaCl_2$] and mixed gently for 5 min). Annexin V binds to this antigen (Phosphatidylserine) on the apoptotic cell surface and fluorochromes (Annexin V-FITC and PI: BD Pharmingen™ FITC Annexin V Apoptosis Detection Kit; cat. no. 556547; BD Biosciences) were used to differentiate between apoptotic and non-viable cells. A total of 5 μl Annexin V-FITC and 5 μl PI was added to the mixture. After 15 min of incubation at ambient temperature (25˚C) in the darkness, the cells were shaken evenly, and within 1 h, flow cytometry was performed to assess cell apoptosis by sorting flow cytometer (BD FACSAria II instrument and computer table; BD Biosciences). Finally, data analysis was conducted using FlowJo software (v10.8.1; FlowJo LLC).

Cell cycle assay. After seeding MCF-7 and MCF-7/TAMR cells in two separate six-well plates at a density of 250,000 cells/well, the control and experimental groups were set up simultaneously. A total of 5 μg/ml BSAPPT was added to the cells in the experimental group. After 8 h, all the cells were collected, centrifuged at 300 x g and 25˚C for 5 min, and the liquid that was left over was discarded. Before the precipitate was centrifuged (300 x g, 25˚C, 5 min), it was washed with 1 ml PBS. The cells were then fully mixed after adding 0.3 ml PBS and 1.2 ml 100% ethanol at -20˚C, and placed in a refrigerator

at -20˚C for 1 h. Centrifugation at 25˚C and 300 x g for 5 min was performed to remove the remaining supernatant, and after reconstitution in 1 ml PBS for 15 min at ambient temperature (25˚C), the cells were centrifuged at 25˚C and 300 x g for 5 min to separate the remaining fluid. Subsequently, the cells were resuspended in 100 μl RNase A reagent and incubated for 30 min at 37˚C. A total of 400 μl PI reagent (50 μg/ml) was then added, thoroughly combined, and incubated at 2-8˚C in a pitch-black environment for 30 min. The specimens were immediately evaluated on the sorting flow cytometer (BD FACSAria II instrument and computer table; BD Biosciences), and red fluorescence was recorded at the excitation wavelength of 488 nm.

Statistical analysis. Data are presented as mean ± standard deviation. GraphPad Prism 8 software (Dotmatics) was used for analysis and plotting of the data. To assess differences between groups in the present study, unpaired Student's t-tests, one-way ANOVA and regression analyses were used. Tukey's post hoc multiple comparisons test was used following ANOVA. FlowJo (v10.8.1; FlowJo LLC) and ImageJ (1.8.0; National Institutes of Health) software were used to process the apoptosis, cell cycle and colony formation images. $P<0.05$ was considered to indicate a statistically significant difference.

Results

BSAPPT strongly inhibits the proliferation of TAM-resistant breast cancer. The molecular formula of PPT is $C_{22}H_{22}O_8$ (19), and BSAPPT is a previously unstudied agent that was obtained from natural products containing PPTs (Fig. 1A). To determine how BSAPPT impacts MCF-7/TAMR cell proliferation, the present study assessed the implications of different dosages (1, 5, 10, 20 and 40 μg/ml) of BSAPPT on the viability of MCF-7, MCF-7/TAMR and MCF-10A cells. The findings demonstrated that BSAPPT significantly inhibited cell proliferation in a concentration-dependent manner after 48 h. The cell viability of MCF-7 and MCF7/TAMR cells treated with 5 μg/ml BSAPPT were 87.40 and 79.05%, respectively, relative to the control group. Compared with the MCF7/TAMR cells, the cell viability of BSAPPT-treated MCF-7 cells was 1.11x stronger (both $P<0.05$; Fig. 1B and C). Furthermore, the cell viability of MCF-7 and MCF-7/TAMR cells treated with 10 μg/ml BSAPPT was 55.09 and 49.55%, respectively, relative to the control group. The cell viability of BSAPPT-treated MCF-7 cells was 1.11-fold greater than that of the MCF7/TAMR cells (both $P<0.05$; Fig. 1B and C). Moreover, the cell vitality of MCF-7 and TAMR cells treated with 20 μg/ml BSAPPT was 48.32 and 41.31%, respectively, relative to the control group. Finally, the cell viability of BSAPPT-treated MCF-7 cells was 1.17-fold greater than that of the MCF7/TAMR cells (both $P<0.05$; Fig. 1B and C).

Half-maximal inhibitory concentration (IC_{50}) analysis demonstrated that, in the presence of BSAPPT, the IC_{50} of MCF-7 cells was 16.94 μg/ml (22.18 μM; Fig. 1D), the IC_{50} of MCF7/TAMR cells was 13.60 μg/ml (17.81 μM; Fig. 1E), and the IC_{50} of MCF-10A cells was 24.25 μg/ml (31.76 μM; Fig. 1F). The IC_{50} of MCF-10A cells was 1.43x that of MCF-7 cells, and 1.78x that of MCF7/TAMR cells. These results demonstrate that the degree of injury caused by BSAPPT in normal mammary gland cells (MCF-10A) was notably less than that in MCF-7 and MCF-7/TAMR cells. In the presence of etoposide (control), the IC_{50} of the MCF-7 cells was 30.20 μg/ml (51.31 μM) (Fig. 1D); the IC_{50} of MCF7/TAMR cells was 45.96 μg/ml (78.09 μM; Fig. 1E); and the IC_{50} of MCF-10A cells was 3.66 μg/ml (6.22 μM; Fig. 1F). This demonstrates that in MCF-7 and MCF-7/TAMR cells, the IC_{50} in the etoposide samples were notably higher than that of the BSAPPT-treated samples; whilst in MCF-10A cells, the IC_{50} of the etoposide group was markedly less than that of the BSAPPT-treated group. These findings indicate that the effective injury concentration of BSAPPT in MCF-7 and MCF-7/TAMR cells was notably lower than that of etoposide, whilst that of BSAPPT in normal cells was markedly greater than that of etoposide. Furthermore, the IC_{50} of BSAPPT-treated A549 and MDA-MB-231 cells was 10.08 and 13.92 μg/ml, respectively (Fig. 1G), thereby confirming that BSAPPT exerted good inhibitory effects on other cancer cell lines.

The role of BSAPPT was subsequently assessed using a colony formation assay, with the aim of determining its effect on the proliferation of the two tumor cell lines, MCF-7 and MCF-7/TAMR. It was demonstrated that 1, 5, 10, 20 and 40 μg/ml BSAPPT resulted in MCF-7 cell relative colony numbers of 91.1, 87.5, 68.6, 48.0 and 40.6, respectively, relative to the normal group ($P<0.05$; Fig. 1H). Furthermore, the MCF-7/TAMR cell relative colony numbers were 90.21, 83.8, 50.79, 39.9 and 31.44, respectively, relative to the control group ($P<0.05$; Fig. 1I). The number of colonies formed by MCF-7 was 1.35, 1.20 and 1.29x that of the MCF-7/TAMR group when the concentrations were 10, 20, and 40 μg/ml, respectively. These data showed that BSAPPT could induce a reduction in both MCF-7 and MCF-7/TAMR colony formation, and that the reduction in colony formation was greater in MCF-7/TAMR than in MCF-7. The aforementioned findings indicate that the process of colony formation was concentration-dependent; that is, the number of colonies formed decreased gradually with increasing drug concentration. Moreover, the results revealed that at doses of 10, 20 and 40 μg/ml, the MCF-7/TAMR cells produced significantly fewer colonies than the MCF-7 cells. The proliferation of TAM-resistant strains was thus significantly more inhibited by BSAPPT than the wild type cells.

BSAPPT exhibits enhanced pro-apoptotic effects in MCF-7/TAMR cells. Many physiologic mechanisms depend on apoptosis, which associated with the onset of several diseases, including cancer, autoimmune disorders and neurological problems (41). To assess whether BSAPPT induces apoptosis in MCF-7 and drug-resistance cells, apoptotic assays were performed. Following a 48-h incubation with 5 μg/ml BSAPPT to MCF-7 and MCF7/TAMR cells, the morphological alterations and characteristics of the cells were evaluated under a light microscope. It was demonstrated that MCF-7 and drug-resistance cells treated with BSAPPT had notably more floating dead cells than those in the control group. Furthermore, it was observed that a markedly greater proportion of cells showed characteristics of apoptosis, such as cytoplasmic condensation, cell division and the formation of apoptotic bodies (Fig. 2A). This indicates that BSAPPT can induce the death of MCF-7 and MCF7/TAMR cells, and PPT derivatives have

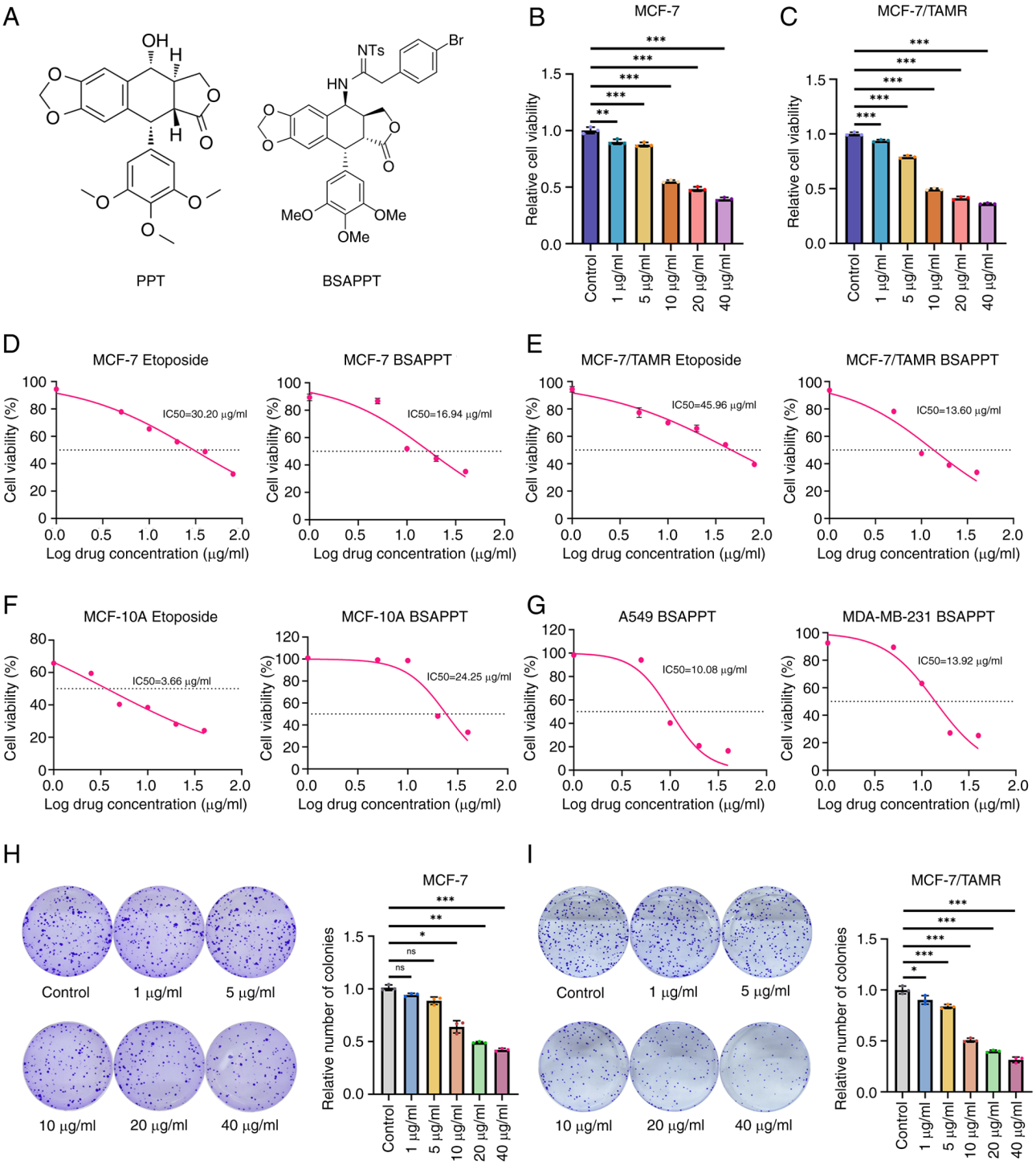

Figure 1. Effect of BSAPPT on MCF-7 and MCF7/TAMR cell viability and proliferation. (A) Organic chemical structural formulas of PPT ($C_{22}H_{22}O_8$) and BSAPPT. Changes in (B) MCF-7 and (C) MCF7/TAMR cell viability after treatment with multiple BSAPPT concentrations. Changes in (D) MCF-7, (E) MCF7/TAMR and (F) MCF-10A cell viability after treatment with varying etoposide and BSAPPT concentrations. (G) Changes in cell viability of A549 and MDA-MB-231 cells after treatment with several BSAPPT doses. Changes in (H) MCF-7 and (I) MCF7/TAMR cell proliferation after treatment with varying concentrations of BSAPPT, and the relative number colonies in each group. *P<0.05; **P<0.01; ***P<0.001. PPT, podophyllotoxin; BSAPPT, bromosulfonamidine amino-PPT; IC_{50}, half-maximal inhibitory concentration; ns, not significant.

been known to cause human tumor cell death (38). Moreover, the apoptosis rates of MCF-7 and MCF7/TAMR cells were assessed using flow cytometry. This was following the cells being left untreated or treated with 5 μg/ml BSAPPT for 48 h to further evaluate the ability of the drug to induce apoptosis in MCF-7 and MCF7/TAMR cells. The results demonstrated that the apoptosis rate of the BSAPPT-treated MCF-7 cell group was 1.44-fold greater in comparison with that of the MCF-7 control group (Fig. 2B). However, the apoptosis rate in the MCF-7/TAMR group receiving treatment was 1.84x higher than that of the MCF-7/TAMR control group (Fig. 2C). In comparison with the MCF-7 cell sample, the apoptosis rate in the MCF-7/TAMR group was 1.28x greater, indicating that the MCF-7/TAMR cells had a notably higher rate of apoptosis

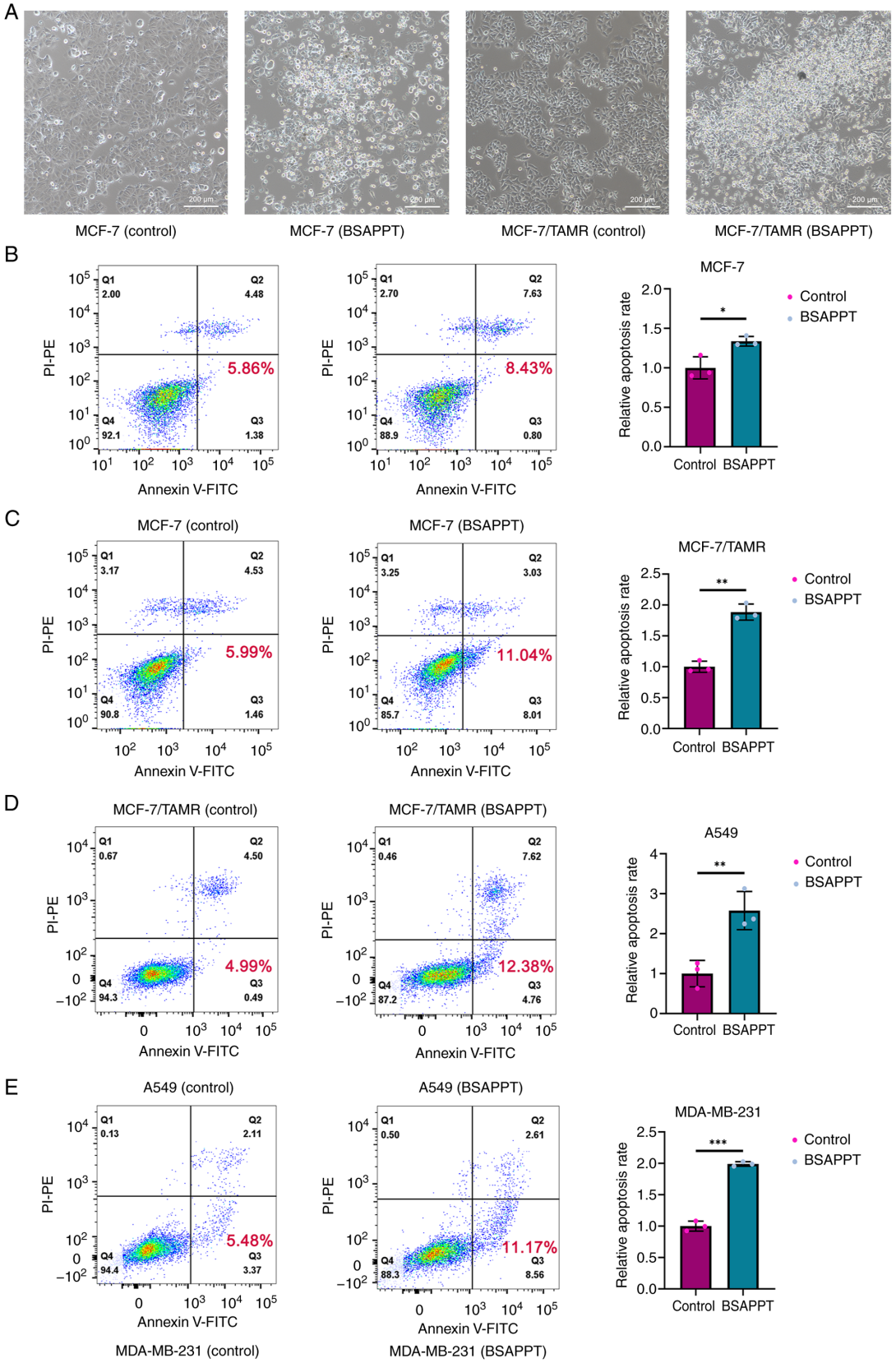

Figure 2. Apoptotic effect of BSAPPT on different cancer cells. (A) Effect of BSAPPT on the morphology of MCF-7 and MCF7/TAMR cells (magnification, x100). Representative flow cytometry graphs demonstrating the changes in the apoptotic rate among (B) MCF-7, (C) MCF7/TAMR, (D) A549 and (E) MDA-MB-231 cells before and after BSAPPT treatment, and the relative apoptosis rate among MCF-7, MCF7/TAMR, A549 and MDA-MB-231 cells in each treatment group compared with control group. *P<0.05; **P<0.01; ***P<0.001. BSAPPT, bromosulfonamidine amino-podophyllotoxin.

following treatment than the MCF-7 cells, which was in concordance with the IC_{50} results. Furthermore, the average apoptotic rate of the MCF-7 group receiving treatment was 1.34x greater than that of the untreated group in three repeated

experiments (both P<0.05), whilst it was 1.89-fold greater in the MCF-7/TAMR treatment group than in the control group (both P<0.05). Therefore, BSAPPT promoted the apoptosis in the MCF-7/TAMR cells by 1.41x more than that in the MCF-7 cells. This indicates that BSAPPT more effectively induced apoptosis in MCF-7/TAMR cells than in MCF-7 cells. Moreover, the apoptosis rate of BSAPPT-treated A549 cells was 2.48x greater than that of the A549 control group (Fig. 2D), and the apoptosis rate of the BSAPPT-treated MDA-MB-231 cells was 2.04-fold greater than that of the MDA-MB-231 control cells (Fig. 2E). The average apoptotic rate of the A549 group receiving treatment was 2.58x greater than that of the untreated group in three repeated experiments (both P<0.05), whilst it was 1.99-fold greater in the MDA-MB-231 treatment sample than in the control sample (both P<0.05). This indicates that BSAPPT also effectively promoted apoptosis in other cancer cells. Thus, BSAPPT may cause apoptosis in other cancer cell lines and induce a greater rate of apoptosis in MCF-7/TAMR cells than in MCF-7 cells.

BSAPPT induces a more significant cell cycle arrest among drug-resistant breast cancer cells. PPT-induced microtubule breakage results in cell cycle arrest during the G_2/M phase, triggering apoptosis (22). Cell cycle evaluation tests were performed to assess the BSAPPT-induced cycle modifications in MCF-7 and MCF-7/TAMR. It was demonstrated that the proportion of MCF-7 in the G_2 phase after 8 h with the addition of 5 μg/ml BSAPPT was 1.41-fold greater than the MCF-7 normal group (Fig. 3A and B). However, after 8 h, the proportion of the MCF-7/TAMR treated with 5 μg/ml BSAPPT during the G_2 phase was 2.13x greater than the MCF-7/TAMR group without treatment (Fig. 3C and D). Furthermore, the proportion of the BSAPPT-treated MCF-7/TAMR group in the G_2 phase was 1.5-fold greater than that of the MCF-7 group. The average ratio of the MCF-7 group in the G_2/M phase was 1.59-fold higher than that of the untreated control group, compared with 1.79-fold greater for the MCF-7/TAMR group receiving treatment compared with the untreated sample (both P<0.05). The mean proportion of the G_2/M phase induced by BSAPPT in MCF-7/TAMR cells was 1.13-fold higher than that in MCF-7 cells. This indicates that BSAPPT more effectively arrests the cell cycle in MCF-7/TAMR cells than in MCF-7 cells, indicating that BSAPPT inhibits cell cycle progression in MCF-7/TAMR cells.

By comparing the untreated group and the drug-treated group, it was demonstrated that the interkinesis of the two untreated groups was markedly longer than that of the division phase; the G_0/G_1 phase >G_2/M phase (Fig. 3E), However, the G_0/G_1 phase interval of the two drug treatment groups was reduced, and BSAPPT induced a 1.6x shortening of G0/G1 phase in MCF-7/TAMR cells compared with MCF-7 cells; consequently, the G_0/G_1 phase was notably shorter in the MCF-7/TAMR cells. Meanwhile, the peak G_2/M phase was markedly higher in the two drug-treated groups, and the G_2/M interval in the MCF-7-treated group was 1.59x greater than the untreated group (P<0.05). The G_2/M interval among the MCF-7/TAMR-treated group was 1.79x greater than that of the control sample (P<0.05). The G_2/M phases of the MCF-7 control sample and the treatment sample differed significantly, and the G_2/M phases of the MCF-7/TAMR control sample and the treatment sample also differed significantly, indicating a cell cycle arrest role of BSAPPT in both the MCF-7 and MCF-7/TAMR cells. The M phase is the spindle assembly checkpoint (42), and the peak G_2/M phase was notably elevated in the drug-treated MCF-7/TAMR group compared with that in the drug-treated MCF-7 group (Fig. 3E). This indicates that BSAPPT may inhibit tubulin binding in both cells. Moreover, BSAPPT may more effectively disrupt the microtubule polymerization of MCF-7/TAMR cells, promoting an increase in the number of cells in the G_2/M state. The cell cycles of both cell lines were inhibited by BSAPPT at the G_2/M period, and the level of G_2/M arrest in the MCF-7/TAMR cells was greater than that in the MCF-7 cells. This indicates a higher degree of inhibition of the drug to MCF-7/TAMR cells. These results reveal that BSAPPT mainly inhibits the G_2/M period in the cell cycle, which consequently leads to the apoptosis of breast cancer cells and inhibits MCF-7/TAMR cell development.

BSAPP regulates the expression of apoptosis and cycle-related genes. The effect of BSAPPT on the expression levels of genes linked to the cell cycle and apoptosis (Bcl-2, Caspase-9, PLK1, PLK4, CCNB1 and TPX2) were assessed using qPCR to gain insight into the molecular mechanisms behind the apoptosis and proliferation restrictions associated with treatment with 10 μg/ml BSAPPT in the MCF-7 and MCF-7/TAMR groups. The results demonstrated that the levels of Bcl-2 expression were significantly upregulated in TAM-resistant cells compared with the MCF-7 group (2.1-fold higher than the original value) and significantly downregulated in MCF-7 and MCF-7/TAMR cells after BSAPPT administration compared with the respective untreated group (82.17 and 70.34%, respectively). Bcl-2 expression reduction was 1.17x greater in MCF-7/TAMR cells than in MCF-7 cells, so the effect was significantly more pronounced in MCF-7/TAMR cells. This indicates that BSAPPT exerted pro-apoptotic effects by inhibiting Bcl-2 expression (Fig. 4A). In contrast, the TAM-resistant cells exhibited a significant reduction in the expression of caspase-9 compared with the MCF-7 group, the gene that initiates apoptosis (43) (76% of the MCF-7 group). Moreover, BSAPPT treatment of MCF-7 and MCF-7/TAMR cells was associated with a significantly upregulated mRNA expression level of caspase-9, which was 1.46x and 1.61x greater, respectively, than in the respective untreated control cells. Moreover, the upregulation of caspase-9 in MCF-7/TAMR cells was 1.10x that in MCF-7 cells. The effect was significantly more pronounced in MCF-7/TAMR cells, indicating that BSAPPT exerts pro-apoptotic effects by promoting the expression of caspase-9 (Fig. 4A).

PLK1, PLK4, CCNB1 and TPX2 are all related genes that regulate the cell cycle: PLK1 is essential for the start, progression and termination of mitosis (44); PLK4 regulates centromere replication during the cell cycle (45); the protein that CCNB1 encodes needs to exist for the proper regulation of the G_2/M transition point during the cell cycle (46); and TPX2 is selectively present in the nucleus throughout the S and G_2 periods inside the cell cycle and is regarded as a critical component connected with cell mitosis and spindle construction (46). These cycle-related genes were significantly more expressed in MCF-7/TAMR cells compared with MCF-7 cells, and both MCF-7 and MCF-7/TAMR cells demonstrated a significant reduction in the expression levels of these genes with BSAPPT

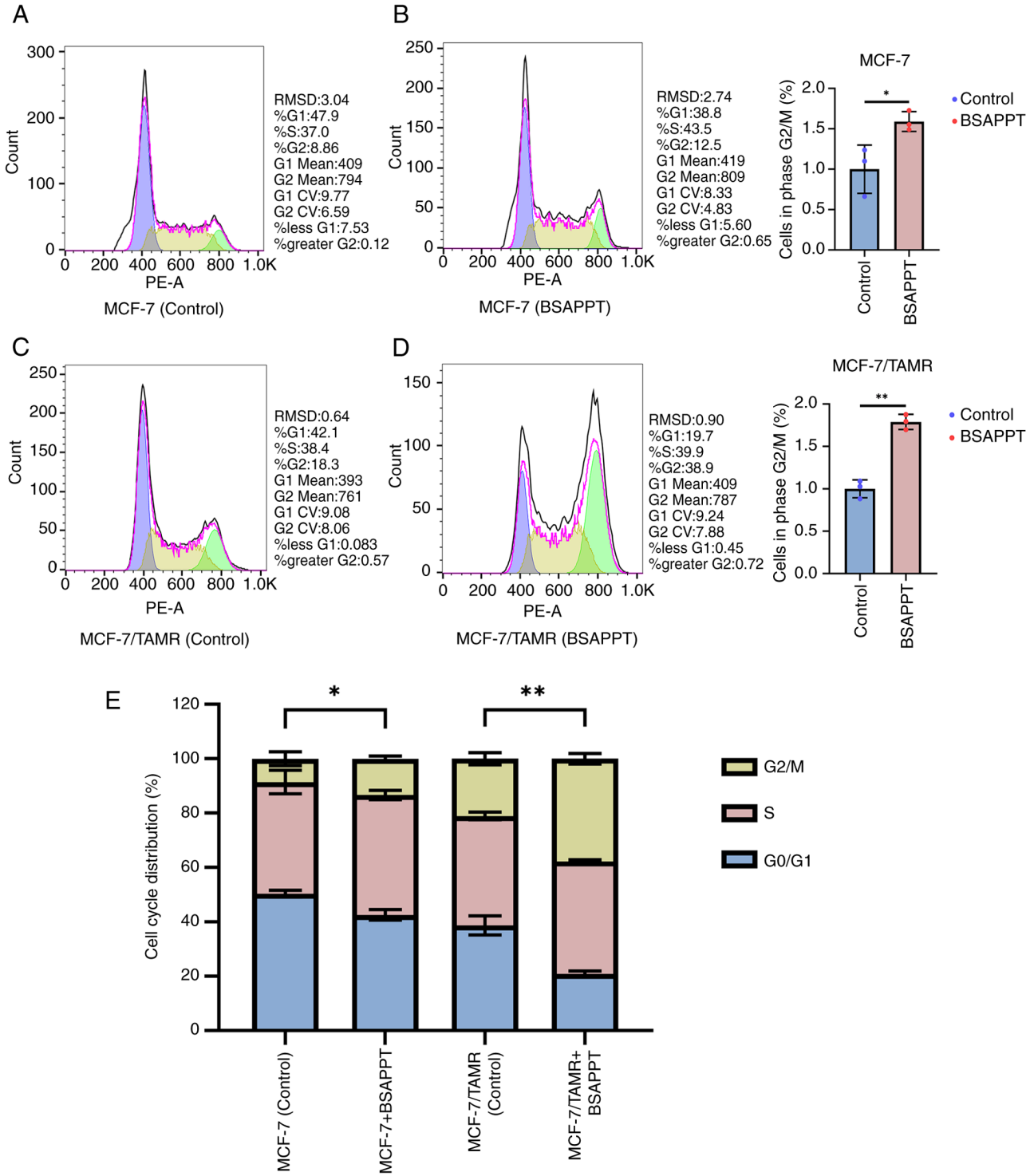

Figure 3. Effect of BSAPPT on the cell cycle in MCF-7 and MCF7/TAMR cells. Changes in the cell cycle of MCF-7 cells when they are (A) left untreated and (B) treated with 5 μg/ml BSAPPT, and the proportion of MCF-7 cells during the G_2/M phase in the two groups. Changes in the cell cycle of MCF7/TAMR cells when they are (C) left untreated and (D) treated with 5 μg/ml BSAPPT, and the proportion of MCF7/TAMR cells in the G_2/M phase in the two groups. (E) Changes in the cycles of MCF-7 and MCF7/TAMR cells before and after administration of 5 μg/ml BSAPPT. *P<0.05; **P<0.01. BSAPPT, bromosulfonamidine amino-podophyllotoxin.

administration compared with the respective untreated control group. Nonetheless, the reduced expression of these genes was significantly more pronounced in MCF-7/TAMR cells than MCF-7 cells (Fig. 4A).

Subsequently, the influence of BSAPPT on the protein levels of Bcl-2, Caspase-9, PLK1, PLK4, CCNB1, and TPX2 were assessed using western blotting. Following 48 h of BSAPPT administration, it was revealed that the protein expression degree of the apoptosis-inhibiting gene, Bcl-2, was markedly increased in MCF-7/TAMR cells compared with that in MCF-7 cells, and in both the MCF-7 and MCF7/TAMR cells, BSAPPT notably reduced Bcl-2 protein expression in treated cells compared with that in respective untreated cells (Fig. 4B); Caspase-9 protein expression was reduced

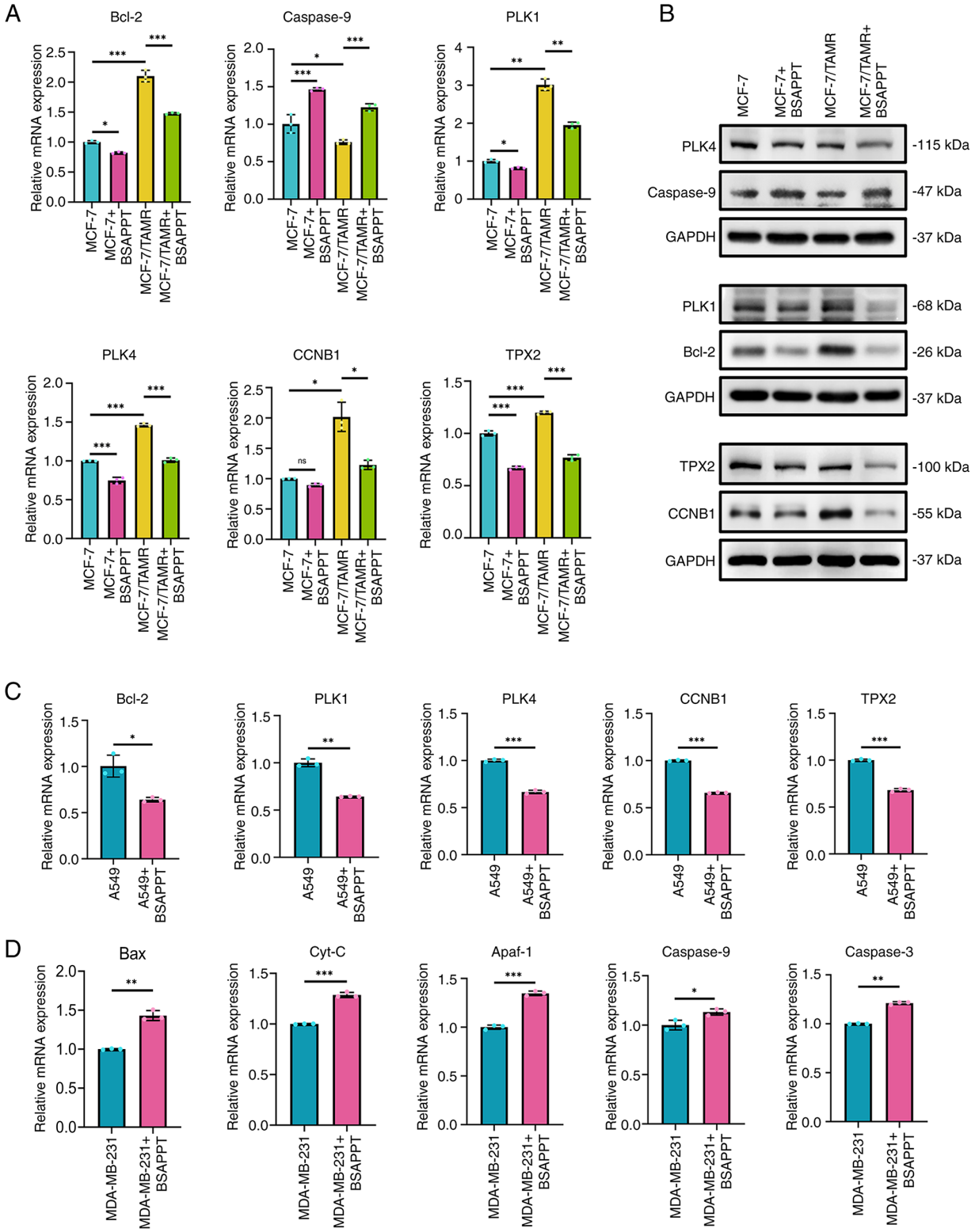

Figure 4. Effect of BSAPPT on apoptosis and cycle-related gene or protein expression in MCF-7, MCF7/TAMR and other cancer cells. (A) mRNA expression levels of genes linked to the cell cycle and apoptosis were measured by qPCR both before and after MCF-7 and MCF7/TAMR cells were treated with 10 μg/ml BSAPPT. (B) Western blotting detection of apoptotic and cycle-related protein expression variations in MCF-7 and MCF7/TAMR cells before and after using 10 μg/ml BSAPPT. Results of qPCR analysis that assessed differences in the level of expression of genes linked to the cell cycle and apoptosis before and after (C) A549 and (D) MDA-MB-231 cells were treated with 10 μg/ml BSAPPT. *P<0.05; **P<0.01; ***P<0.001. BSAPPT, bromosulfonamidine amino-podophyllotoxin; qPCR, quantitative PCR; Bcl-2, B-cell lymphoma 2; Caspase, cysteine aspartic acid-specific protease; PLK, polo like kinase; CCNB1, cyclin B1; TPX2, targeting protein for Xklp2; Bax, Bcl-2 associated X; Cyt-C, cytochrome c; Apaf-1, apoptotic protease activating factor 1.

in MCF-7/TAMR cells compared with that in MCF-7 cells, and BSAPPT administration was associated with a marked increase in expression of Caspase-9 among the treated group compared with that in the respective untreated group in both

the MCF-7 and MCF-7/TAMR cells (Fig. 4B); MCF-7/TAMR cells demonstrated notably elevated levels of PLK1 and CCNB1 protein expression compared with MCF-7 cells, and BSAPPT treatment was associated with a notably reduced levels of PLK1, PLK4, CCNB1 and TPX2 protein expression in treated cells compared with that in respective untreated cells in both MCF-7 and MCF7/TAMR cells (Fig. 4B).

Upon assessing the molecular mechanism of BSAPPT in other tumor cell lines, it was observed that BSAPPT administration was associated with a significant reduction in the relative gene expression of Bcl-2, PLK1, PLK4, CCNB1 and TPX2 in A549 cells to 63.77, 64.29, 66.60, 65.82 and 68.00, respectively, compared with untreated groups (all $P<0.05$; Fig. 4C). Bcl-2 associated X (Bax) is an apoptosis-promoting gene and a water-soluble related protein homolog of Bcl-2, belonging to the Bcl-2 gene family. It undermines the protective function of Bcl-2, often resulting in cell death and the emergence of cytochrome *c* (Cyt C) (47). Cyt-C is a key molecule involved in apoptosis. When cells are stimulated by apoptotic signals, released Cyt-C from the mitochondria forms an apoptotic complex with apoptotic protease activating factor (Apaf)-1 protein with the assistance of deoxyadenosine triphosphate and the caspase-recruiting structural domain at the amino-terminus of Apaf-1 in the apoptotic complex will recruit Pro-Caspase-9 to form activated Caspase-9. Apoptosis is induced by Caspase-3, which is activated by Caspase-9 (43,48,49). In the present study, BSAPPT administration was associated with a significant increase in the relative levels of gene expression of Caspase-9, Cyt-C, Apaf-1, Caspase-3 and Bax in MDA-MB-231 cells by 1.13-, 1.29-, 1.35-, 1.21- and 1.43-fold, respectively, compared with untreated cells (all $P<0.05$; Fig. 4D).

Discussion

Most patients with ER^+ breast cancer receive endocrine therapy, including TAM, and although certain patients respond well to TAM, the risk of resistance and recurrence remains (6). PPT has been of interest for its broad-spectrum and highly potent antitumor, antiviral, antibacterial and immunosuppressive activities, as well as its antiproliferative activity in many types of cancers (36), but no studies related to PPT drugs targeting MCF-7/TAMR cells have been reported, to the best of our knowledge. Although semi-synthetic derivatives of PPT have antineoplastic properties, their clinical use is limited due to their high toxicity, increased cancer cell resistance, uncontrolled release, poor water solubility, low bioavailability and increased myelosuppression and cytotoxicity to normal human cells (50,51). To improve the efficiency and lower the side effects of PPT, more PPT-based derivatives were developed (52). The present study investigated a completely new, unstudied derivative, BSAPPT, and the demonstrated that BSAPPT reverses the malignant phenotype of MCF-7/TAMR cells by inhibiting their proliferation.

It was revealed that BSAPPT exhibited a concentration-dependent effect on the inhibition of MCF-7 and MCF-7/TAMR cell development, and the degree of injury to MCF-10A cells was less than that in MCF-7 and MCF-7/TAMR cells. Furthermore, the results demonstrated that the extent of injury to MCF-10A cells by etoposide was greater than that by BSAPPT. Therefore, the small degree of injury caused by BSAPPT to normal human cells is advantageous. In both MCF-7 and MCF-7/TAMR cells, BSAPPT effectively increased the rate of apoptosis, with a greater degree of apoptosis in the MCF-7/TAMR cells. This concurs with a previous report stating that the main molecular mechanism underlying the antineoplastic effect of ghrelin included the trigger of apoptosis (20), which is characterized by nuclear chromatin condensation and fragmentation, dense cytoplasmic organelles, endoplasmic reticulum expansion and phagocytosis of apoptotic cells (43). Moreover, the G_2/M stage of the MCF-7/TAMR cell cycle was inhibited by BSAPPT, thereby inducing the apoptosis of MCF-7/TAMR cells and inhibiting the development of MCF-7/TAMR, which agrees with results from a previous study that reported that, in a dose-dependent manner, PPT may stop SGC-7901 cells from proliferating and trigger their apoptosis, resulting in cell cycle block during the G_2/M phase (53). The inhibition by BSAPPT in the MCF-7 cell cycle was not as significant as that in the MCF-7/TAMR cells. Additionally, it was demonstrated that BSAPPT notably decreased the rate of cell division by promoting apoptosis in several types of cells, including MDA-MB-231 and A549 cells.

The Bcl-2-regulated apoptotic pathway is associated with carcinogenesis and could be a useful target for future medication progress (47). The present research demonstrated that drug-resistant cells express Bcl-2 at high levels, and the downregulation of Bcl-2 promoted apoptosis in MCF-7 and MCF7/TAMR cells after BSAPPT therapy. This agrees with the findings of a previous study that reported that a critical variation in the acquisition of TAM resistance in MCF-7/TAMR is the promotion of proliferation and reduction of apoptosis through Bcl-2 regulation (54). The results are also in concordance with a previous study that reported that overexpression of the Bcl-2 protein was associated with several malignancies, including breast cancer (55). Furthermore, the present research demonstrated that MCF-7/TAMR cells expresses caspase-9 at low levels, and the activation of caspase-9 can promote apoptosis in MCF-7 and MCF-7/TAMR cells with BSAPPT treatment. This agrees with the findings of a previous study which reported that inhibition of caspase-9 led to attenuation of the apoptosis, resulting in increased migration, proliferation and invasion of breast cancer cells (56). Lastly, the activation of the caspase family and effector caspases is caused by certain apoptosis-inducing stimuli (57). Caspase-9 of the intrinsic or mitochondrial apoptotic pathway is a protease that initiates apoptosis and is triggered by a multi-protein triggering platform, which later induces apoptotic signals through the activation of caspase-3 and -7, and then their role triggers apoptosis in many cell lines (43).

Cell cycle proteins are vital for regulating the length of the cell cycle (58). According to results of the present research, MCF-7/TAMR cells displayed increased protein expressions of PLK1 and CCNB1.The decreased protein expressions of PLK1, CCNB1, PLK4 and TPX2 were associated with the action of BSAPPT, which is consistent with the findings of a previous study that reported that the overexpression of PLK1 and CCNB1 was associated with a reduced survival rate of patients with breast cancer, indicating their potentiality as prognostic markers (59). Meanwhile, a mitogenic protein, CCNB1, is an essential cell cycle regulator at the G_2/M

checkpoint and serves a role in the oncogene route of several malignancies, including colon cancer and breast cancer (46). A previous study indicated that the level of expression of PLK1 and PLK4 was greater within breast cancer tissue compared with healthy normal tissues, and increased levels of PLK1 and PLK4 in breast malignant tissue induced the stimulation of breast cancer carcinogenesis; however, their association with breast cancer-resistant cells was not studied (60). The level of expression of TPX2 is tightly regulated by the cell cycle (61); however, a previous study reported that TPX2 was markedly increased in different stages of breast cancer, and the low overall survival of many patients with cancer is associated with its excessive expression (46). These cycle proteins block the progression of the cell cycle of MCF-7 and MCF-7/TAMR cells, leading to proliferation inhibition of MCF-7 and MCF-7/TAMR cells. Otherwise, the degree of blockage in the MCF-7/TAMR cells was greater than that in the MCF-7 cells. Moreover, the present study revealed that the mRNA levels of Bcl-2, PLK1, PLK4, CCNB1 and TPX2 in A549 cells were significantly decreased following BSAPPT administration, which is consistent with the trends of mRNA expression within MCF-7 and MCF-7/TAMR cells, when treated cells are compared with untreated cells. However, MDA-MB-231 cells had higher mRNA levels of Bax, Cyt-C, Apaf-1, Caspase-9 and Caspase-3 in drug-treated cells compared with untreated cells, which may be because the MDA-MB-231 cells underwent apoptosis due to an alteration in the Cyt-C/Apaf-1/Caspase-9/Caspase-3 route activation. This agrees with a previous study, which reported that within human multiple myeloma cells, the Cyt-C/Apaf-1/Caspase-9/Caspase-3 signaling cascade caused cell death (48). Overall, the results of the present research indicate that BSAPPT causes apoptosis and G_2/M stage cell cycle block, which therefore suppresses the growth of MCF-7/TAMR cells in a dose-dependent manner.

In summary, the creation of a novel class of PPT-derived compounds with enhanced cytotoxicity and selectivity against cancer cells is motivated by the adverse effects and broad-spectrum anticancer capabilities of PPT as an anti-neoplastic drug (36). The present study demonstrated that BSAPPT promotes apoptosis in TAM-resistant breast cancer cells by downregulating Bcl-2, upregulating Caspase-9 and inhibiting the cell cycle of MCF-7/TAMR cells through the downregulation of PLK1, PLK4, CCNB1 and TPX2, which inhibits the development of breast cancer tumors. This indicates that BSAPPT exerts a suppressive role in TAM resistance in breast tumors, thereby revealing potential for the inhibition and control of breast cancer involving TAM resistance as well as providing strategies for the therapy of other cancers; however, more in-depth investigations are needed to verify this. Moreover, it is uncertain if BSAPPT acts on the colchicine binding site on microtubule proteins to prevent microtubule proteins from assembling into mitotic spindle microtubules. This is a major limitation of the present study, and further investigations should be performed related to microtubule proteins.

Acknowledgements

Not applicable.

Funding

The present study was supported by the Guangzhou and Dongguan Joint Fund Cultivation Project (grant nos. 2021B 1515140002 and 2023A1515140033) and the PhD Research Start-Up Fund Project (grant no. DBBS2023001).

Availability of data and materials

The data generated in the present study may be requested from the corresponding author.

Authors' contributions

YZ conceived and designed the study. FL performed the drug screening and cycle experiments. JW was the primary contributor to the composition of the manuscript, whilst also performing all other experiments and data analysis. XL and BZ participated in the design of the study and reviewed the work critically for important intellectual content. JW, XL and BZ confirm the authenticity of all the raw data. All authors have read and approved the final version of the manuscript. All authors agreed to be accountable for all aspects of the work in ensuring that questions related to the accuracy or integrity of any part of the work are appropriately investigated and resolved.

Ethics approval and consent to participate

Not applicable.

Patient consent for publication

Not applicable.

Competing interests

The authors declare that they have no competing interests.

References

1. Shen Y, Zhong J, Liu J, Liu K, Zhao J, Xu T, Zeng T, Li Z, Chen Y, Ding W, *et al*: Protein arginine N-methyltransferase 2 reverses tamoxifen resistance in breast cancer cells through suppression of ER-α36. Oncol Rep 39: 2604-2612, 2018.
2. Mishra A, Srivastava A, Pateriya A, Tomar MS, Mishra AK and Shrivastava A: Metabolic reprograming confers tamoxifen resistance in breast cancer. Chem Biol Interact 347: 109602, 2021.
3. Sung H, Ferlay J, Siegel RL, Laversanne M, Soerjomataram I, Jemal A and Bray F: Global cancer statistics 2020: GLOBOCAN estimates of incidence and mortality worldwide for 36 cancers in 185 countries. CA Cancer J Clin 71: 209-249, 2021.
4. Jin ML, Kim YW, Jin HL, Kang H, Lee EK, Stallcup MR and Jeong KW: Aberrant expression of SETD1A promotes survival and migration of estrogen receptor α-positive breast cancer cells. Int J Cancer 143: 2871-2883, 2018.
5. Ring A and Dowsett M: Mechanisms of tamoxifen resistance. Endocr Relat Cancer 11: 643-658, 2004.
6. Shi Q, Li Y, Li S, Jin L, Lai H, Wu Y, Cai Z, Zhu M, Li Q, Li Y, *et al*: LncRNA DILA1 inhibits Cyclin D1 degradation and contributes to tamoxifen resistance in breast cancer. Nat Commun 11: 5513, 2020.
7. Zhu Y, Liu Y, Zhang C, Chu J, Wu Y, Li Y, Liu J, Li Q, Li S, Shi Q, *et al*: Tamoxifen-resistant breast cancer cells are resistant to DNA-damaging chemotherapy because of upregulated BARD1 and BRCA1. Nat Commun 9: 1595, 2018.

8. Lüönd F, Sugiyama N, Bill R, Bornes L, Hager C, Tang F, Santacroce N, Beisel C, Ivanek R, Bürglin T, *et al*: Distinct contributions of partial and full EMT to breast cancer malignancy. Dev Cell 56: 3203-3221.e11, 2021.
9. Tufail M, Cui J and Wu C: Breast cancer: Molecular mechanisms of underlying resistance and therapeutic approaches. Am J Cancer Res 12: 2920-2949, 2022.
10. Yin L, Zhang XT, Bian XW, Guo YM and Wang ZY: Disruption of the ER-α36-EGFR/HER2 positive regulatory loops restores tamoxifen sensitivity in tamoxifen resistance breast cancer cells. PLoS One 9: e107369, 2014.
11. Hosford SR and Miller TW: Clinical potential of novel therapeutic targets in breast cancer: CDK4/6, Src, JAK/STAT, PARP, HDAC, and PI3K/AKT/mTOR pathways. Pharmgenomics Pers Med 7: 203-215, 2014.
12. Li D, Ji H, Niu X, Yin L, Wang Y, Gu Y, Wang J, Zhou X, Zhang H and Zhang Q: Tumor-associated macrophages secrete CC-chemokine ligand 2 and induce tamoxifen resistance by activating PI3K/Akt/mTOR in breast cancer. Cancer Sci 111: 47-58, 2020.
13. Mansouri S, Farahmand L, Teymourzadeh A and Majidzadeh AK: Clinical evidence on the magnitude of change in growth pathway activity in relation to tamoxifen resistance is required. Curr Cancer Drug Targets 18: 668-676, 2018.
14. Viedma-Rodriguez R, Baiza-Gutman L, Salamanca-Gomez F, Diaz-Zaragoza M, Martinez-Hernandez G, Ruiz Esparza-Garrido R, Velázquez-Flores MA and Arenas-Aranda D: Mechanisms associated with resistance to tamoxifen in estrogen receptor-positive breast cancer (review). Oncol Rep 32: 3-15, 2014.
15. Gao A, Sun T, Ma G, Cao J, Hu Q, Chen L, Wang Y, Wang Q, Sun J, Wu R, *et al*: LEM4 confers tamoxifen resistance to breast cancer cells by activating cyclin D-CDK4/6-Rb and ERα pathway. Nat Commun 9: 4180, 2018.
16. Cai F, Xiao H, Sun Y, Wang D and Tang J: Expression of Snail and E-cadherin in Drug-resistant MCF-7/ADM breast cancer cell strains. J Coll Physicians Surg Pak 29: 240-244, 2019.
17. Vesuna F, Bergman Y and Raman V: Genomic pathways modulated by Twist in breast cancer. BMC Cancer 17: 52, 2017.
18. Joseph C, Alsaleem M, Orah N, Narasimha PL, Miligy IM, Kurozumi S, Ellis IO, Mongan NP, Green AR and Rakha EA: Elevated MMP9 expression in breast cancer is a predictor of shorter patient survival. Breast Cancer Res Treat 182: 267-282, 2020.
19. Shah Z, Gohar UF, Jamshed I, Mushtaq A, Mukhtar H, Zia-Ui-Haq M, Toma SI, Manea R, Moga M and Popovici B: Podophyllotoxin: History, recent advances and future prospects. Biomolecules 11: 603, 2021.
20. Hong WG, Cho JH, Hwang SG, Lee E, Lee J, Kim JI, Um HD and Park JK: Chemosensitizing effect of podophyllotoxin acetate on topoisomerase inhibitors leads to synergistic enhancement of lung cancer cell apoptosis. Int J Oncol 48: 2265-2276, 2016.
21. Guerram M, Jiang ZZ and Zhang LY: Podophyllotoxin, a medicinal agent of plant origin: Past, present and future. Chin J Nat Med 10: 161-169, 2012.
22. Xiao J, Gao M, Sun Z, Diao Q, Wang P and Gao F: Recent advances of podophyllotoxin/epipodophyllotoxin hybrids in anticancer activity, mode of action, and structure-activity relationship: An update (2010-2020). Eur J Med Chem 208: 112830, 2020.
23. Ma Y, Fang S, Li H, Han C, Lu Y, Zhao Y, Liu Y and Zhao C: Biological evaluation and molecular modelling study of podophyllotoxin derivatives as potent inhibitors of tubulin polymerization. Chem Biol Drug Des 82: 12-21, 2013.
24. Zhang X, Rakesh KP, Shantharam CS, Manukumar HM, Asiri AM, Marwani HM and Qin HL: Podophyllotoxin derivatives as an excellent anticancer aspirant for future chemotherapy: A key current imminent needs. Bioorg Med Chem 26: 340-355, 2018.
25. Renouard S, Lopez T, Hendrawati O, Dupre P, Doussot J, Falguieres A, Ferroud C, Hagege D, Lamblin F, Laine E and Hano C: Podophyllotoxin and deoxypodophyllotoxin in Juniperus bermudiana and 12 other Juniperus species: Optimization of extraction, method validation, and quantification. J Agric Food Chem 59: 8101-8107, 2011.
26. Yu X, Xu T, Su B, Zhou J, Xu B, Zhang Y, Zhu Y, Jiang N and He Z: The novel role of etoposide in inhibiting the migration and proliferation of small cell lung cancer and breast cancer via targeting Daam1. Biochem Pharmacol 210: 115468, 2023.
27. Orr MS, Fornari FA, Randolph JK and Gewirtz DA: Transcriptional down-regulation of c-myc expression in the MCF-7 breast tumor cell line by the topoisomerase II inhibitor, VM-26. Biochim Biophys Acta 1262: 139-145, 1995.
28. Sledge GW Jr: Etoposide in the management of metastatic breast cancer. Cancer 67 (Suppl 1): S266-S270, 1991.
29. Cabel L, Carton M, Cheaib B, Pierga JY, Dalenc F, Mailliez A, Levy C, Jacot W, Debled M, Leheurteur M, *et al*: Oral etoposide in heavily pre-treated metastatic breast cancer: Results from the ESME cohort and comparison with other chemotherapy regimens. Breast Cancer Res Treat 173: 397-406, 2019.
30. Alpsoy A, Yasa S and Gündüz U: Etoposide resistance in MCF-7 breast cancer cell line is marked by multiple mechanisms. Biomed Pharmacother 68: 351-355, 2014.
31. Hartmann JT and Lipp HP: Camptothecin and podophyllotoxin derivatives: Inhibitors of topoisomerase I and II-mechanisms of action, pharmacokinetics and toxicity profile. Drug Saf 29: 209-230, 2006.
32. Allen TM and Cullis PR: Drug delivery systems: Entering the mainstream. Science 303: 1818-1822, 2004.
33. Carstensen H, Nolte H and Hertz H: Teniposide-induced hypersensitivity reactions in children. Lancet 2: 55, 1989.
34. Chu B, Shi S, Li X, Hu L, Shi L, Zhang H, Xu Q, Ye L, Lin G, Zhang N and Zhang X: Preparation and evaluation of teniposide-loaded polymeric micelles for breast cancer therapy. Int J Pharm 513: 118-129, 2016.
35. Nielsen D, Boas J, Engelholm SA, Hansen OP and Dombernowsky P: Teniposide in advanced breast cancer. A phase II trial in patients with no prior chemotherapy. Ann Oncol 3: 377-378, 1992.
36. Zi CT, Yang L, Xu FQ, Dong FW, Yang D, Li Y, Ding ZT, Zhou J, Jiang ZH and Hu JM: Synthesis and anticancer activity of dimeric podophyllotoxin derivatives. Drug Des Devel Ther 12: 3393-3406, 2018.
37. Pujol MD, Romero M and Sánchez I: Synthesis and biological activity of new class of dioxygenated anticancer agents. Curr Med Chem Anticancer Agents 5: 215-237, 2005.
38. Yang TM, Qi SN, Zhao N, Yang YJ, Yuan HQ, Zhang B and Jin S: Induction of apoptosis through caspase-independent or caspase-9-dependent pathway in mouse and human osteosarcoma cells by a new nitroxyl spin-labeled derivative of podophyllotoxin. Apoptosis 18: 727-738, 2013.
39. Siegel RL, Miller KD, Wagle NS and Jemal A: Cancer statistics, 2023. CA Cancer J Clin 73: 17-48, 2023.
40. Livak KJ and Schmittgen TD: Analysis of relative gene expression data using real-time quantitative PCR and the 2(-Delta Delta C(T)) Method. Methods 25: 402-408, 2001.
41. Han HW, Lin HY, He DL, Ren Y, Sun WX, Liang L, Du MH, Li DC, Chu YC, Yang MK, *et al*: Novel podophyllotoxin derivatives as potential tubulin inhibitors: Design, synthesis, and antiproliferative activity evaluation. Chem Biodivers 15: e1800289, 2018.
42. Qin X, Zhang Y, Yu H and Ma L: Progress in the Study of spindle assembly checkpoint in lung cancer. Zhongguo Fei Ai Za Zhi 26: 310-318, 2023 (In Chinese).
43. Kim B, Srivastava SK and Kim SH: Caspase-9 as a therapeutic target for treating cancer. Expert Opin Ther Targets 19: 113-127, 2015.
44. Liu Z, Sun Q and Wang X: PLK1, A potential target for cancer therapy. Transl Oncol 10: 22-32, 2017.
45. Zhao Y and Wang X: PLK4: A promising target for cancer therapy. J Cancer Res Clin Oncol 145: 2413-2422, 2019.
46. Chen G, Yu M, Cao J, Zhao H, Dai Y, Cong Y and Qiao G: Identification of candidate biomarkers correlated with poor prognosis of breast cancer based on bioinformatics analysis. Bioengineered 12: 5149-5161, 2021.
47. Yamaguchi H, Paranawithana S, Lee M, Huang Z, Bhalla K, Wang HG. Yamaguchi H, Paranawithana SR, Lee MW, Huang Z, *et al*: Epothilone B analogue (BMS-247550)-mediated cytotoxicity through induction of Bax conformational change in human breast cancer cells. Cancer Res 62: 466-471, 2002.
48. Li Z, Guo D, Yin X, Ding S, Shen M, Zhang R, Wang Y and Xu R: Zinc oxide nanoparticles induce human multiple myeloma cell death via reactive oxygen species and Cyt-C/Apaf-1/Caspase-9/Caspase-3 signaling pathway in vitro. Biomed Pharmacother 122: 109712, 2020.

49. Yadav N, Gogada R, O'Malley J, Gundampati RK, Jayanthi S, Hashmi S, Lella R, Zhang D, Wang J, Kumar R, *et al*: Molecular insights on cytochrome c and nucleotide regulation of apoptosome function and its implication in cancer. Biochim Biophys Acta Mol Cell Res 1867: 118573, 2020.
50. Li M, Zhao Y, Sun J, Chen H, Liu Z, Lin K, Ma P, Zhang W, Zhen Y, Zhang S and Zhang S: pH/reduction dual-responsive hyaluronic acid-podophyllotoxin prodrug micelles for tumor targeted delivery. Carbohydr Polym 288: 119402, 2022.
51. Paidakula S, Nerella S, Vadde R, Kamal A and Kankala S: Design and synthesis of 4β-Acetamidobenzofuranone-podophyllotoxin hybrids and their anti-cancer evaluation. Bioorg Med Chem Lett 29: 2153-2156, 2019.
52. Zhao W, Cong Y, Li HM, Li S, Shen Y, Qi Q, Zhang Y, Li YZ and Tang YJ: Challenges and potential for improving the druggability of podophyllotoxin-derived drugs in cancer chemotherapy. Nat Prod Rep 38: 470-488, 2021.
53. Ji CF and Ji YB: Apoptosis of human gastric cancer SGC-7901 cells induced by podophyllotoxin. Exp Ther Med 7: 1317-1322, 2014.
54. Jeong D, Ham J, Kim HW, Kim H, Ji HW, Yun SH, Park JE, Lee KS, Jo H, Han JH, *et al*: ELOVL2: A novel tumor suppressor attenuating tamoxifen resistance in breast cancer. Am J Cancer Res 11: 2568-2589, 2021.
55. Dawson SJ, Makretsov N, Blows FM, Driver KE, Provenzano E, Le Quesne J, Baglietto L, Severi G, Giles GG, McLean CA, *et al*: BCL2 in breast cancer: A favourable prognostic marker across molecular subtypes and independent of adjuvant therapy received. Br J Cancer 103: 668-675, 2010.
56. Zhang L, Zhang X, Wang X, He M and Qiao S: MicroRNA-224 promotes tumorigenesis through downregulation of caspase-9 in triple-negative breast cancer. Dis Markers 2019: 7378967, 2019.
57. Frenzel A, Labi V, Chmelewskij W, Ploner C, Geley S, Fiegl H, Tzankov A and Villunger A: Suppression of B-cell lymphomagenesis by the BH3-only proteins Bmf and Bad. Blood 115: 995-1005, 2010.
58. Goodger NM, Gannon J, Hunt T and Morgan PR: Cell cycle regulatory proteins-an overview with relevance to oral cancer. Oral Oncol 33: 61-73, 1997.
59. Fang L, Liu Q, Cui H, Zheng Y and Wu C: Bioinformatics analysis highlight differentially expressed CCNB1 and PLK1 genes as potential anti-breast cancer drug targets and prognostic markers. Genes (Basel) 13: 654, 2022.
60. Jiawei W, Xiajun B, Tian S, Xuzheng G and Zhenwang Z: Comprehensive analysis of PLKs expression and prognosis in breast cancer. Cancer Genet 268-269: 83-92, 2022.
61. Ma S, Rong X, Gao F, Yang Y and Wei L: TPX2 promotes cell proliferation and migration via PLK1 in OC. Cancer Biomark 22: 443-451, 2018.